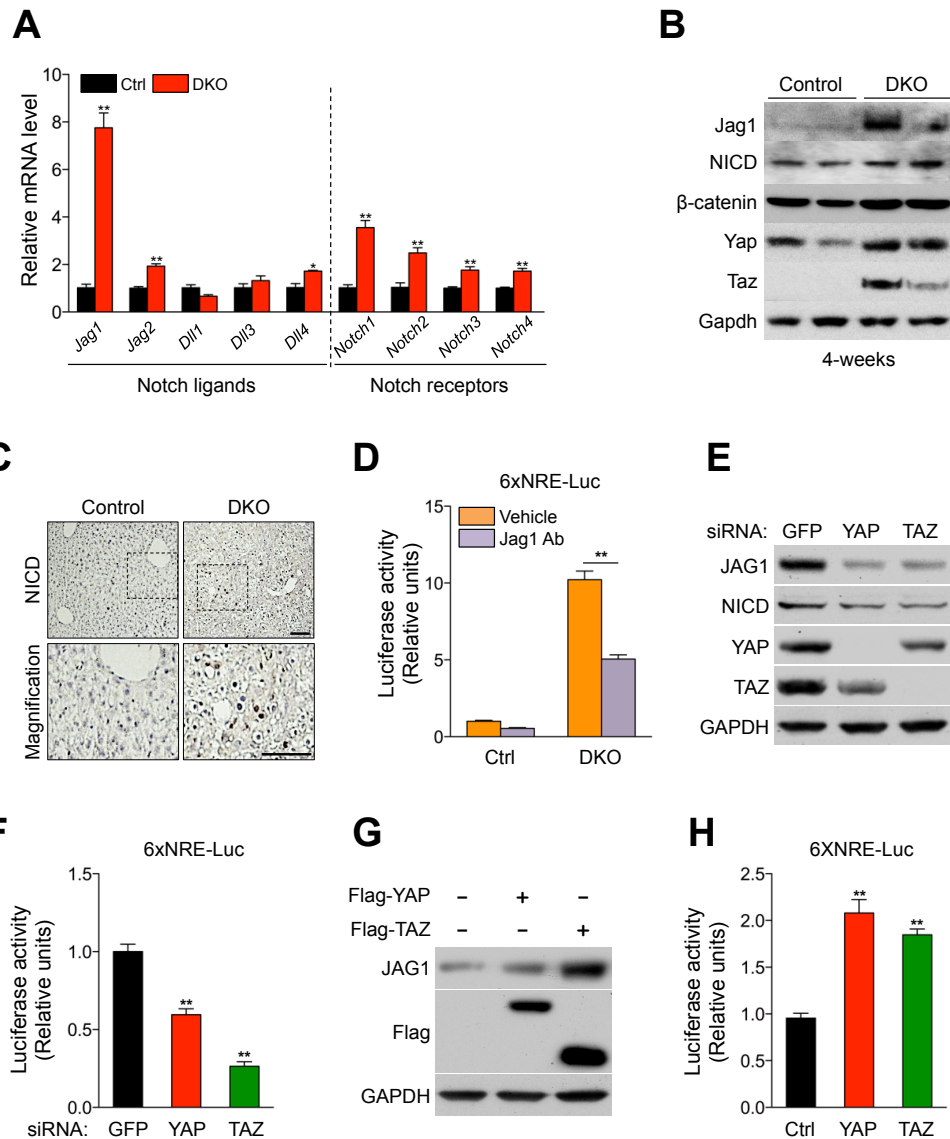


Supplemental Material

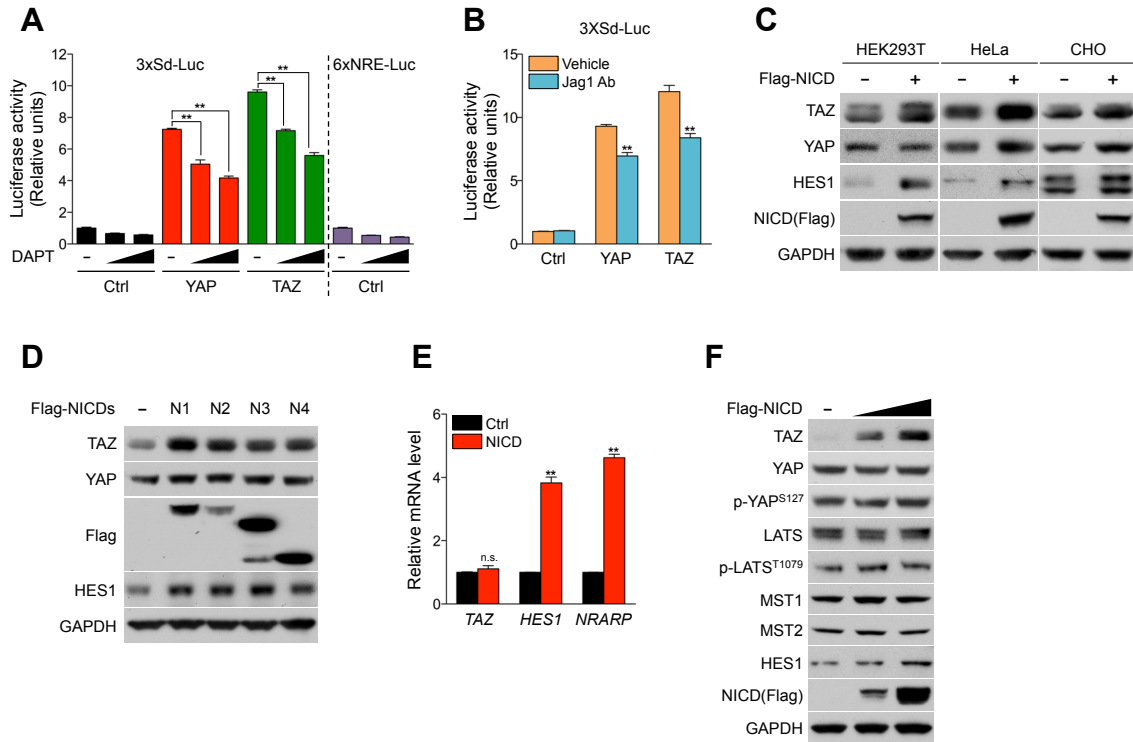
**Interacting Network of Hippo, Wnt/ β -catenin and Notch
Signaling Represses Liver Tumor Formation**

Wantae Kim, Sanjoy Kumar Khan, Jelena Gvozdenovic-Jeremic, Youngeun Kim, Jason
Dahlman, Hanjun Kim¹, Ogyi Park, Tohru Ishitani, Eek-hoon Jho, Bin Gao, Yingzi Yang

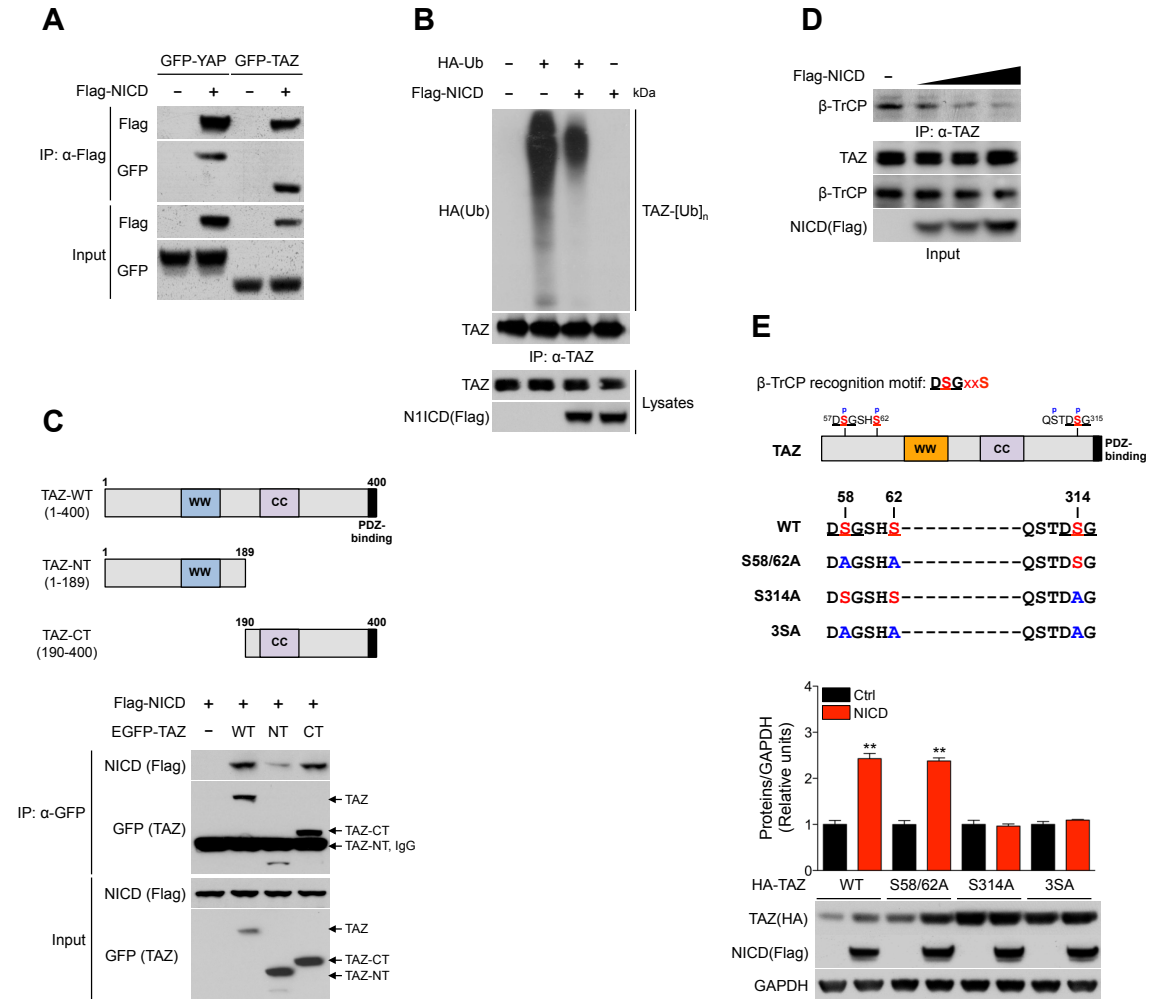
Twelve Supplemental Figures



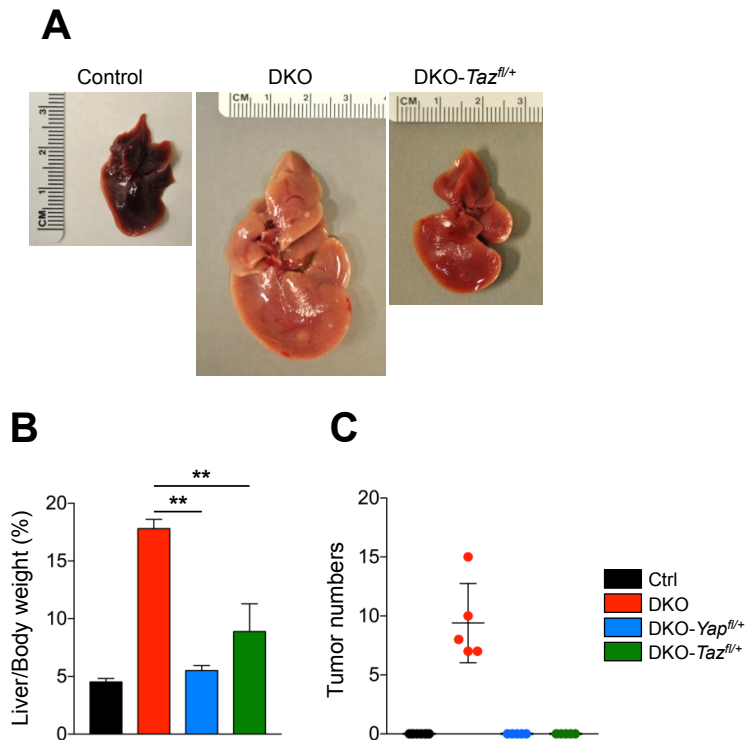
Supplementary Figure 1. Yap/Taz activates Notch signaling. (A) qRT-PCR analysis of Notch ligand (*Jagged1/2* and *Delta-like1/2/4*) and receptor gene (*Notch 1-4*) expression in 2-month old control and DKO liver (n=3). (B) Western blot analysis of liver tissue lysates from 4 weeks old control and DKO mice. (C) A representative IHC of NICD in liver from 4-month-old control and DKO mice. Scale bars, 100 μ m. (D) Notch-reporter activities in the primary DKO mouse hepatocytes was reduced by treating with the neutralizing Jag1 antibody (15 μ g/ml) (n=3). (E and F) Western blot analysis (E) and Notch-dependent reporter assay (F) in YAP or TAZ knocking down or control Huh7 cells (n=3). (G and H) Western blot analysis of indicated protein (G) and Notch-dependent reporter assay (H) in Huh7 cells transiently expressing YAP or TAZ (n=3). Data are expressed as the mean \pm SEM. ** $P < 0.01$, by 2-tailed Student's *t* test (A and D) and 1-way ANOVA with Tukey's post-hoc test (F and H) when ANOVA was significant.



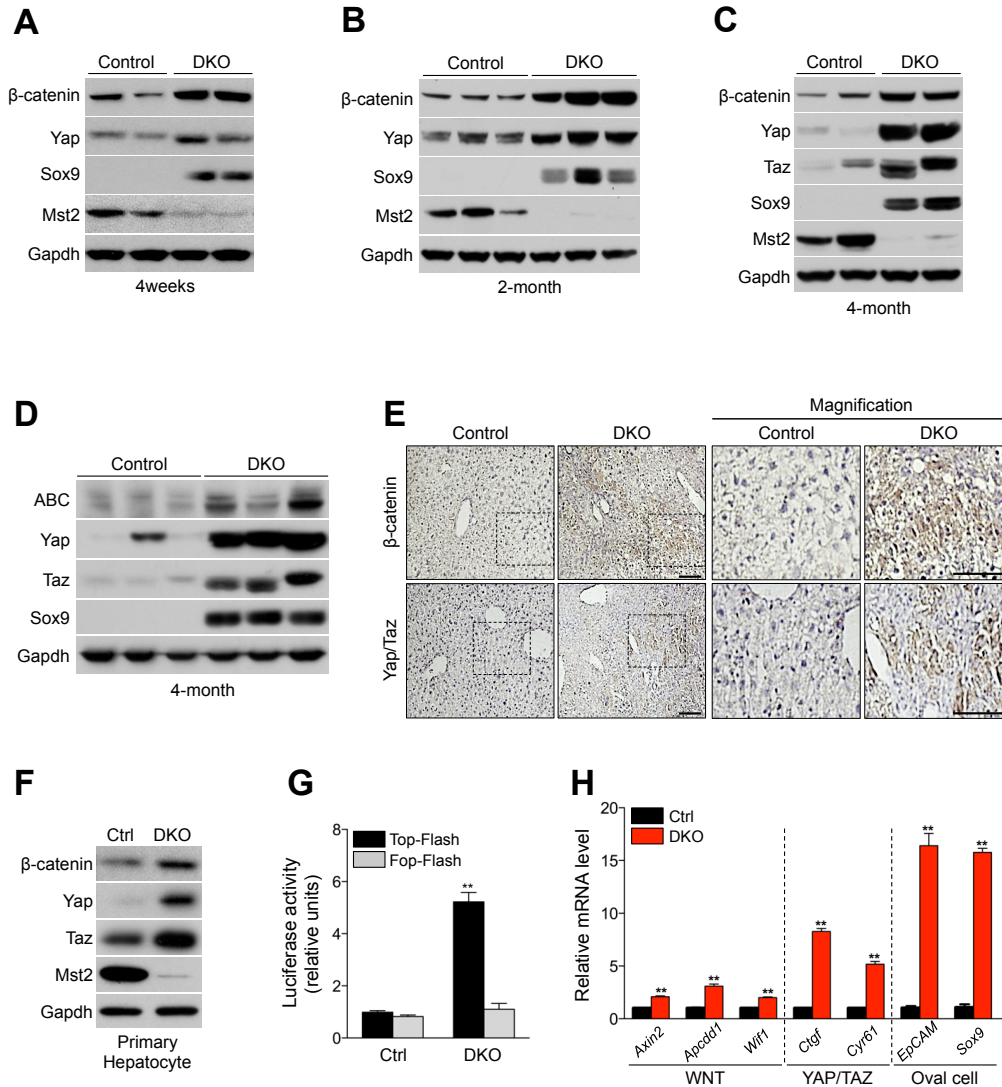
Supplementary Figure 2. Notch signaling enhances YAP/TAZ activity. (A) DAPT, γ -secretase inhibitor, reduces YAP/TAZ-dependent reporter activity. Huh7 cells were transiently transfected with indicated plasmid. 24 hours after transfection, cells were treated with 25 μ M or 50 μ M DAPT. (B) Analysis of YAP or TAZ-mediated reporter activities by treatment with Jag1 antibody (15 μ g/ml) in Huh7 cells transiently expressing YAP or TAZ. (C) Western blot analysis of different cell lines, including HEK293T, HeLa and CHO with or without NICD expression. (D) Western analysis of TAZ protein in Huh7 cells expressing four different Notch intracellular domains. (E) qRT-PCR analysis of indicated gene expression in Huh7 cells expressing NICD (n=3). (F) Notch signaling does not alter Hippo signaling as determined by phosphor-YAP and -LATS. Data are expressed as the mean \pm SEM. ** $P < 0.01$, by 2-tailed Student's t test.



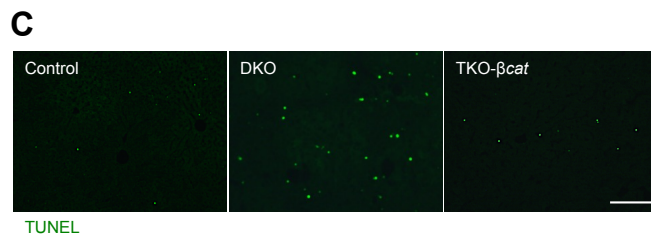
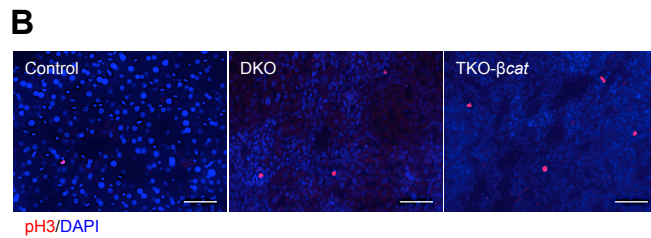
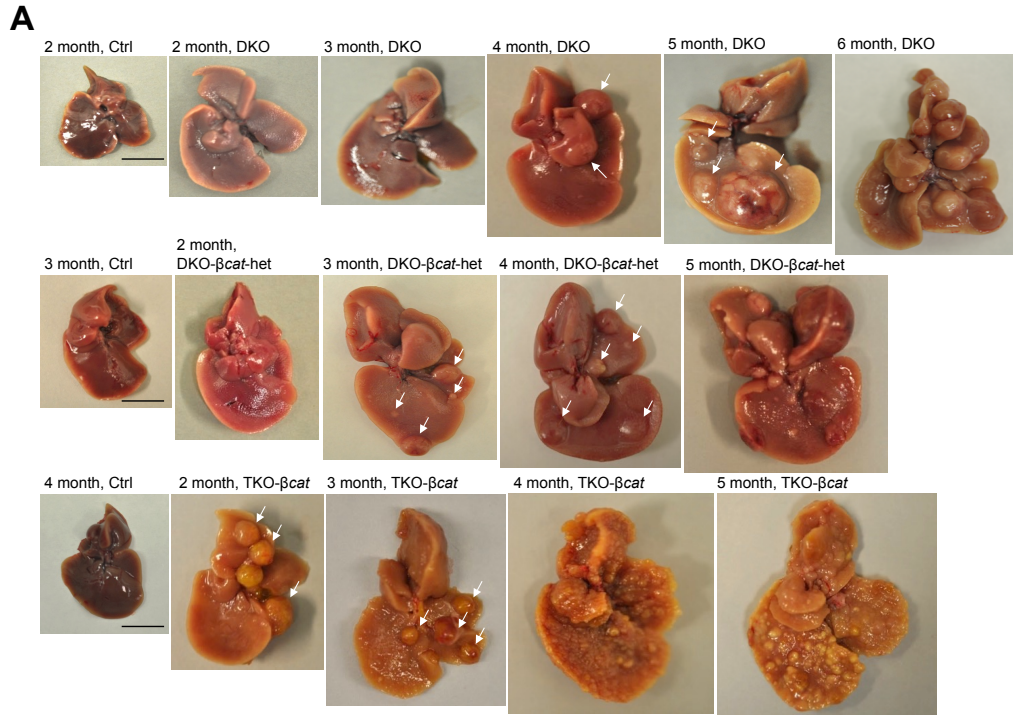
Supplementary Figure 3. Notch Intracellular Domain (NICD) interacts with YAP/TAZ and prevents it from β -TrCP binding. (A) GFP-YAP or -TAZ was transfected together with or without Flag-tagged NICD into Huh7 cells. 24 hours after transfection, cells were treated with 20 μ M MG132 for 8hr, and then lysates were immunoprecipitated with anti-Flag antibody. (B) HA-Ubiquitin was transfected with or without Flag-tagged NICD, and then lysates from Huh7 cells treated with 20 μ M MG132 for 8hr were immunoprecipitated with anti-TAZ antibody and analyzed by Western blotting. (C) Schematic diagrams describing TAZ deletion constructs used in IP assay (upper panel). Domain mapping study revealed that C-terminal region of TAZ is required for binding to NICD (bottom panel). (D) IPed TAZ in NICD-expressing cells shows dose-dependently decrease in interaction with β -TrCP. (E) Schematic diagram showing two β -TrCP recognition sites in TAZ and its mutant constructs (upper panel). Comparison of the TAZ mutant protein levels regulated by NICD expression. Quantification of protein expression by Western blotting was shown in the bottom panel (n=3 per group). Data are expressed as the mean \pm SEM. ***P* < 0.01, by 2-tailed Student's *t* test.



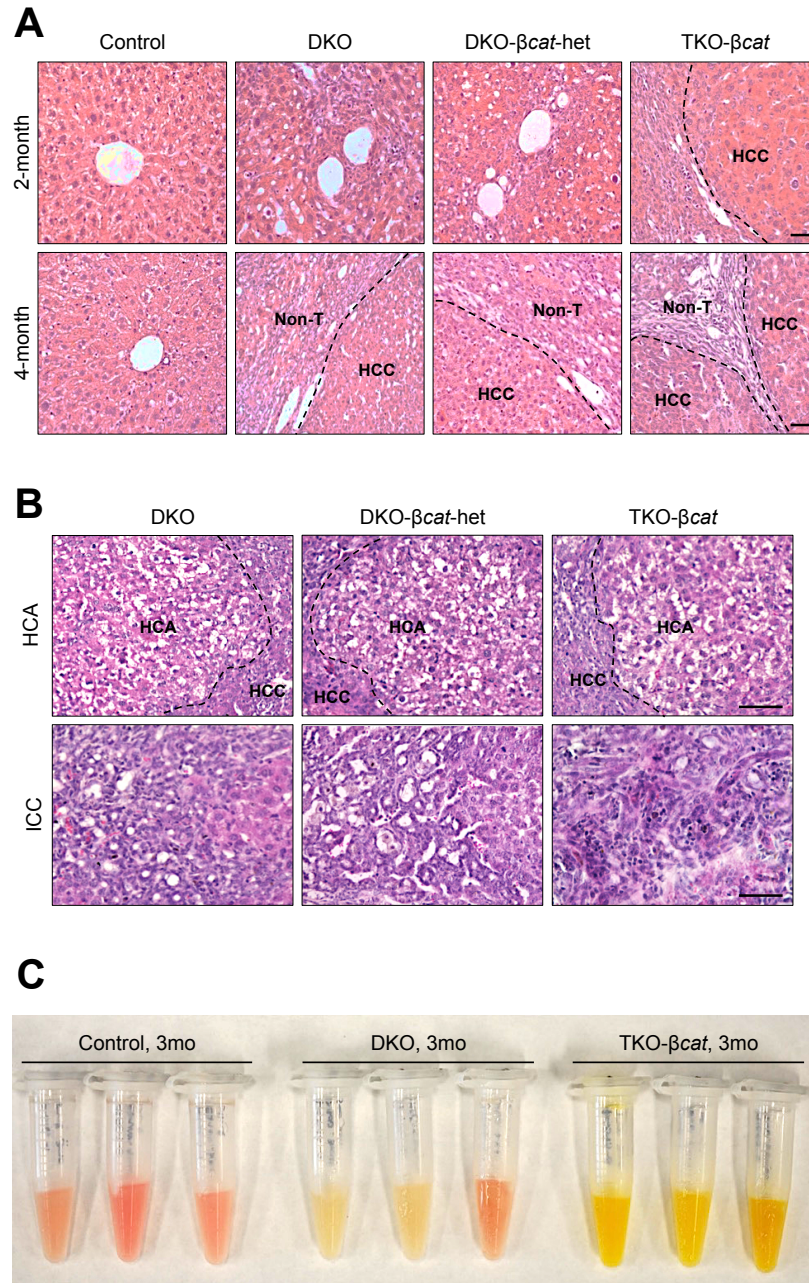
Supplementary Figure 4. Removal of one allele of *Taz* is sufficient to restore DKO liver phenotypes. (A-C) Representative macroscopic appearances of liver (A) and analysis of liver-to-body weight ratio (B) and tumor number (C) from 4 months old mice with indicated genotypes. (n=5-8). Data are expressed as the mean \pm SD. $**P < 0.01$, by 1-way ANOVA with Tukey's post-hoc test.



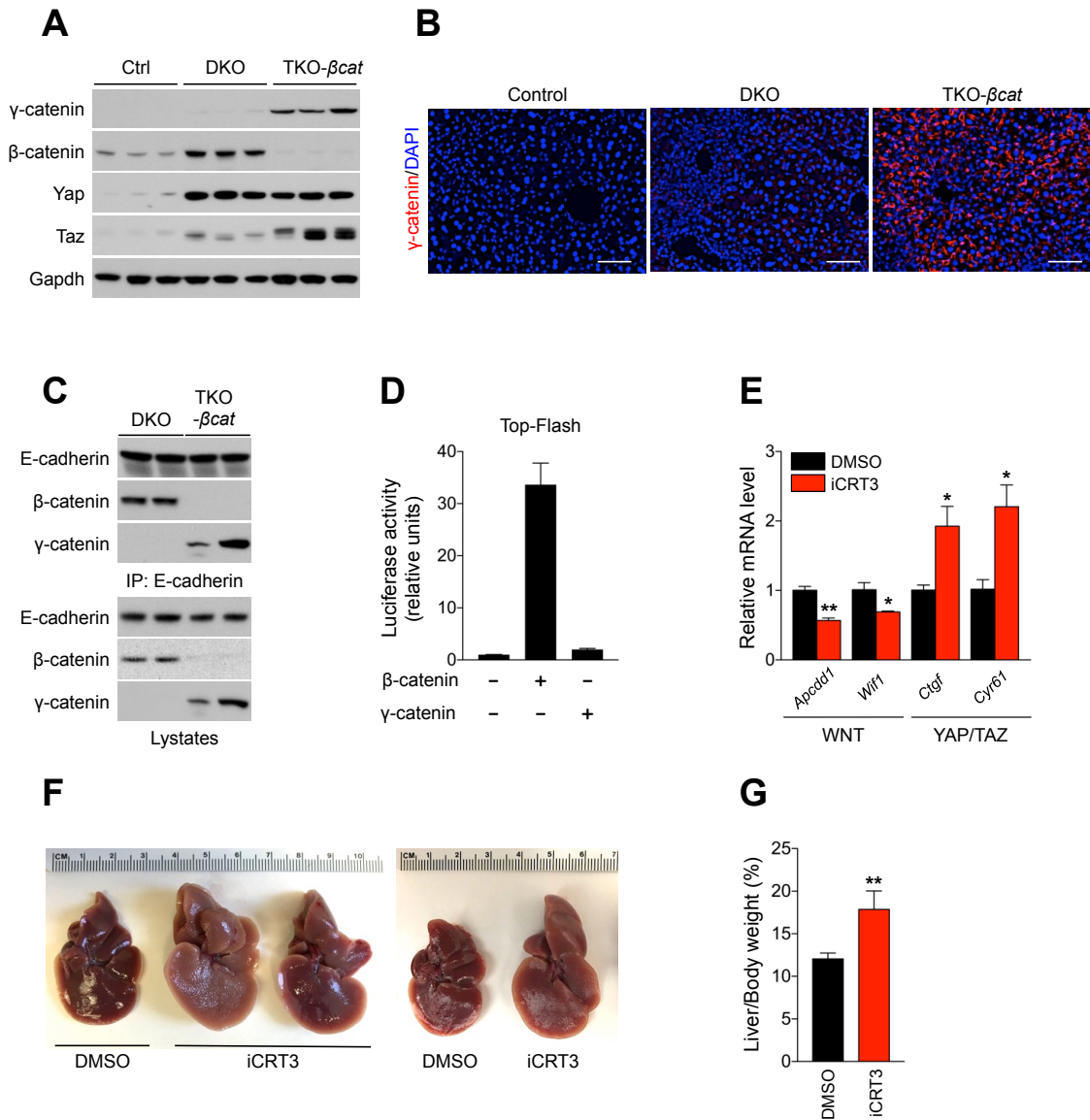
Supplementary Figure 5. β-Catenin is up-regulated in DKO liver by modulating β-TrCP expression. (A-C) Western blot analysis of control and DKO liver lysates from different age group of mice. Gapdh serves as loading control. (D) Western blot analysis of liver extracts from control and DKO mice at 4 months of age using antibodies against active β-catenin (ABC), Yap, Taz and Sox9. (E) Representative images of liver section immunohistochemistry (IHC) with β-catenin or Yap/Taz antibodies. Scale bars, 100μm. (F) Western blotting analysis of indicated proteins in primary hepatocytes isolated from 2 months old control and DKO mice. (G) Significant induction of β-catenin-dependent reporter activity (Top-Flash) in primary hepatocyte from DKO. Fop-Flash used as a negative control (n=3). (H) qRT-PCR of Wnt-target genes, Yap/Taz-target genes and oval cell markers between control and DKO liver (n=3). Data are expressed as the mean ± SEM. ** $P < 0.01$, by 2-tailed Student's t test.



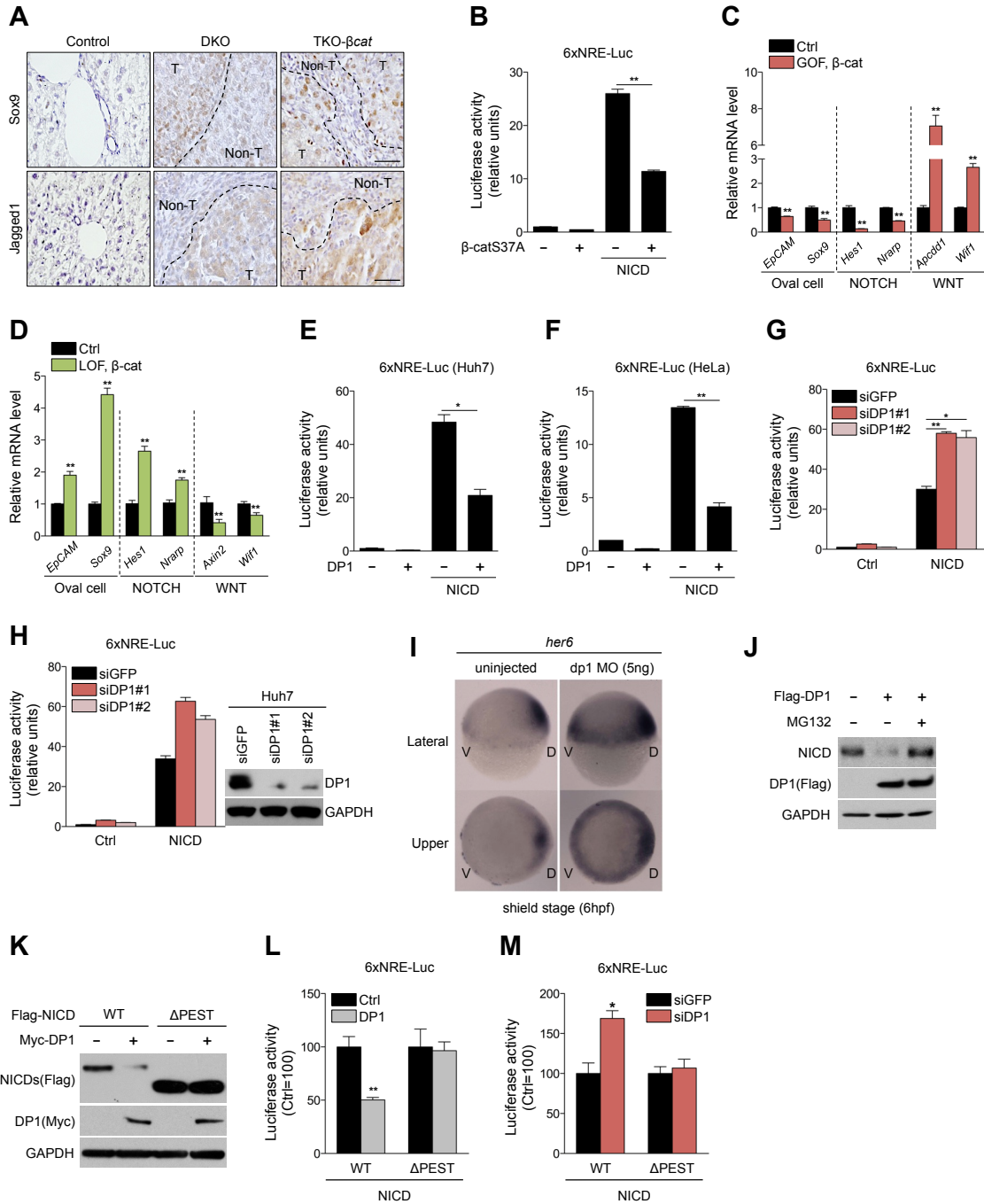
Supplementary Figure 6. Loss of β -catenin in DKO promotes liver enlargement and tumor development. (A) Representative macroscopic appearances of livers from mice with indicated ages and genotypes. Arrows point to tumors. Size bars indicate 1cm. (B) Immunofluorescence staining for phosphor-Histone3 (pSer10) in indicated mouse liver tissue. Scale bars, 100 μ m. (C) Immunofluorescence staining of TUNEL-positive cells with indicated mouse liver tissue. Scale bars, 200 μ m.



Supplementary Figure 7. Removal of β -Catenin promotes tumor initiation and malfunction. (A) Representative hematoxylin and eosin (H&E)-stained liver sections from mice with the indicated ages and genotypes. Dot lines represent the boundaries between adjacent non-tumor region and HCCs at 2 and 4 months of age. Scale bars, 50 μ m. (B) Representative H&E-stained ICCs and HCAs from mice with the indicated genotypes. Dot lines represent the boundaries between adjacent HCAs and HCCs (C) Comparison of serum color from mice with indicated genotypes and ages. Serum from DKO and TKO mouse liver exhibits yellow color due to elevation of bilirubin levels.

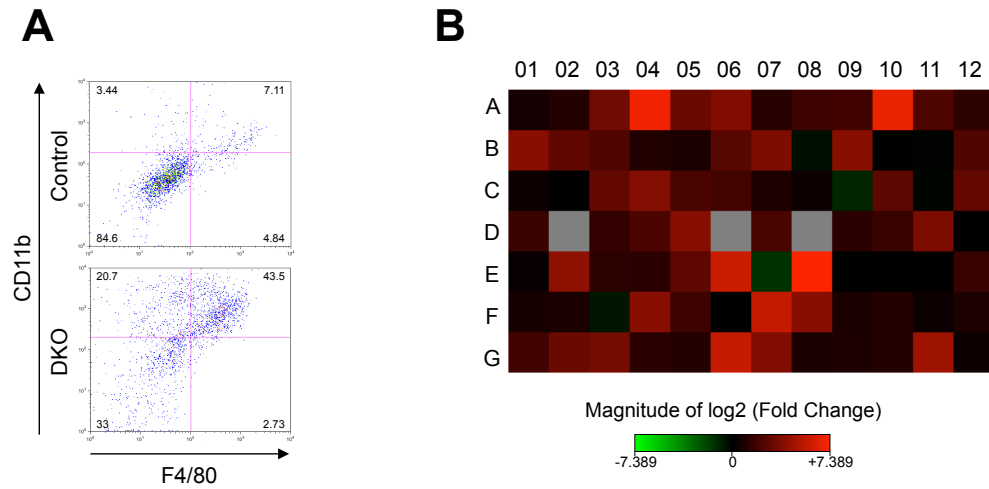


Supplementary Figure 8. Transcriptional role of β -catenin is required for Yap/Taz activities. (A) Western blotting analysis of liver lysates from 4months old control, DKO and TKO- β cat mice. (B) Liver cross-sections from 6week old mice were subjected to IF staining with anti- γ -catenin antibody. Size bar, 100 μ m. (C) IP was performed using anti-E-cadherin, and co-precipitated was analyzed by Western blotting. (D) Augment of Top-Flash activity by β -catenin, but not by γ -catenin in Huh7 cells. (E) DKO mice received 20 IP injection of iCRT3 at a concentration of 20mg/kg every other day or the vehicle DMSO. qRT-PCR analysis of Wnt/ β -catenin or Yap target genes expression in liver samples of 4 months old mice (n=3). (F) Representative macroscopic appearance of livers treated with DMSO or iCRT3. (G) Quantitative analysis of liver-to-body weight ratio (n=5 for DMSO and n=4 for iCRT3). Data are expressed as the mean \pm SEM. * $P < 0.05$, ** $P < 0.01$, by 2-tailed Student's t test.



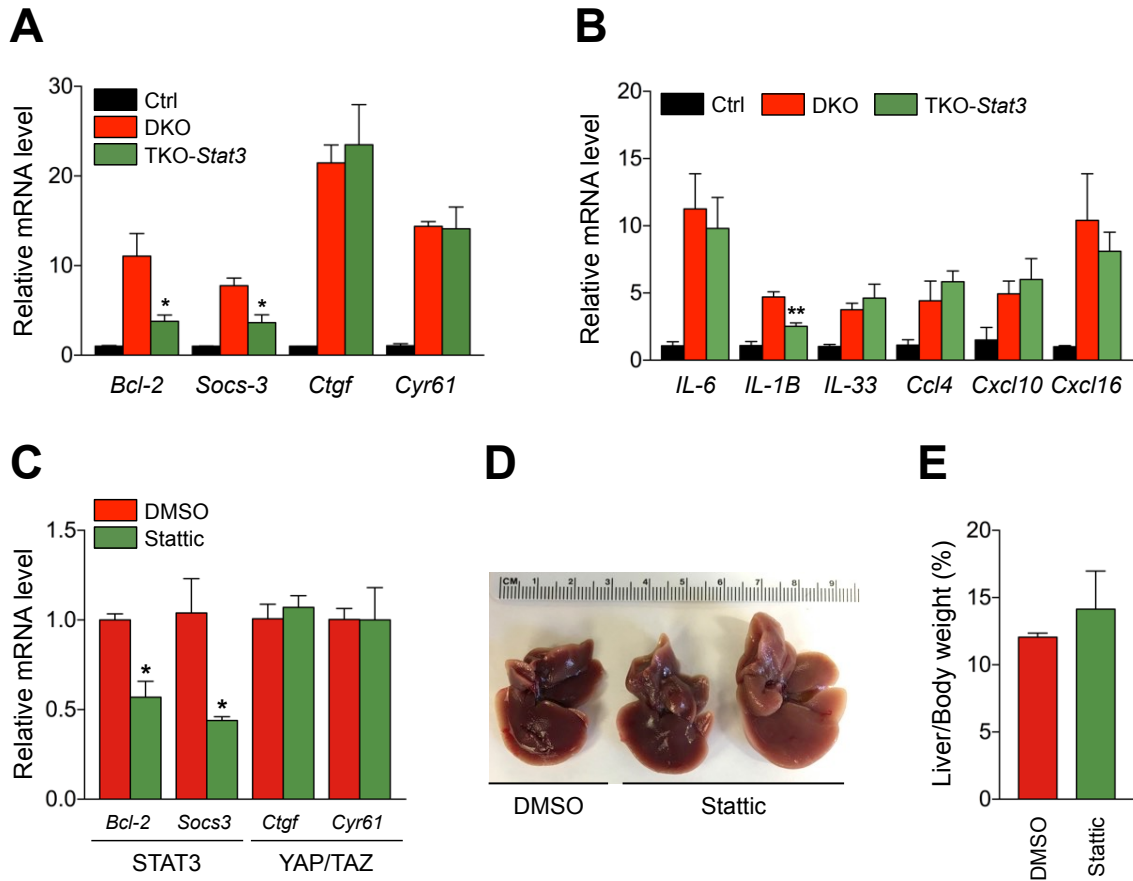
Supplementary Figure 9. β-Catenin signaling inhibits Notch pathway in liver of Mst1/2 DKO mice by regulating DP1 localization. (A) Representative IHC of Sox9 or Jag1 in liver from indicated mice. Dashed line indicates boundary between tumor nodules and non-tumor regions. Scale bars, 50μm. (B) Suppression of NICD-mediated reporter activity by β-catenin-S37A expression (n=3). (C and D) qRT-PCR analysis of expression of oval cell markers, Notch or Wnt target genes (n=3). (E and F) Suppression of NICD-mediated reporter activity by ectopic expression of DP1 in Huh7 (E) or HeLa (F) cells

(n=3). (**G** and **H**) Enhancement of NICD-mediated reporter activity in DP1 knocking down HeLa (**G**) or Huh7 (**H**) cells (n=3). Efficient knockdown of DP1 expression was shown by Western blotting on the right. (**I**) Depletion of zebrafish Dp1 by morpholino (MO) induces expression of Notch target gene *her6* in early stage of zebrafish embryo. (**J**) Huh7 cells was transfected with siGFP or siDP1 RNA, and then analyzed by Western blotting using antibodies indicated. MG132 treatment was done at 20 μ M for 8 hours. (**K**) Western blotting analysis for NICD or NICD Δ PEST protein with or without DP1 expression in Huh7 cells. (**L** and **M**) Notch reporter activities were measured in cells transfected with indicated plasmids (**L**) or siDP1 (**M**). Data are expressed as the mean \pm SEM. * $P < 0.05$, ** $P < 0.01$, by 2-tailed Student's *t* test.

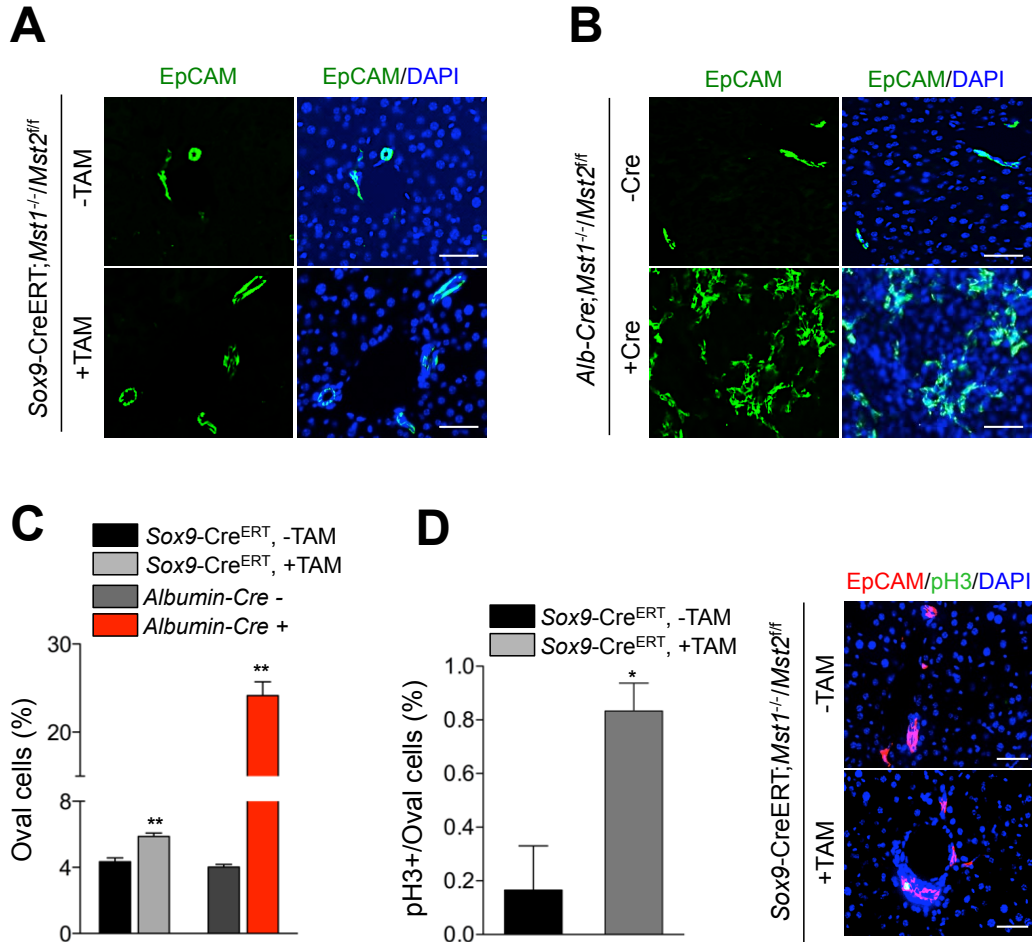


Layout	01	02	03	04	05	06	07	08	09	10	11	12
A	Akt1	Bax	Bcl2	Ccl12	Ccl3	Ccl4	Ccl5	Cd4	Cd40	Cd40lg	Cd80	cdc25a
B	Cdkn1a	Cebpd	Csf1	Csf2	Csf3	Csf3r	Cxcl10	Cxcl12	Cxcr4	Egfr	Fas	Fasl
C	Hgf	Ikbbk	Il10	Il11	Il12a	Il13	Il15	Il17a	Il18	Il18r1	Il1a	Il1b
D	Il1r1	Il2	Il21	Il22	Il23a	Il24	Il2ra	Il3	Il4	Il5	Il6	Il6ra
E	Il6st	Il7	Il9	Jak2	Jak3	Lif	Lifr	Lta	Map2k1	Mapk1	Mapk14	Mapk3
F	Mapk8	Met	Mtor	Myc	Nfkb	Nfkbia	Osm	Osmr	Pias3	Pim1	Rac1	Rela
G	Socs1	Socs3	Src	Stat3	Tir4	Tnf	Tnfrsf10b	Tnfrsf1a	Tnfrsf1b	Tnfsf10	Tnfsf11	Tyk2

Supplementary Figure 10. IL6/Stat3 signaling is activated in DKO mice liver. (A) Single-cell suspension of control and DKO liver cells were subjected to flow cytometry to identify subset of Kupffer cells. (B) Heat maps representing the significantly upregulated (red) and downregulated (green) genes in the DKO liver when compared with control mice liver.



Supplementary Figure 11. Stat3 inhibition has no influence on DKO liver phenotypes. (A) qRT-PCR analysis of Yap or Stat3 target genes expression in liver samples of 4 months old mice (n=3, mean \pm SEM, * P < 0.05). (B) qRT-PCR analysis of cytokine and chemokine gene expression in liver samples of 4 months old mice indicated genotyping (n=3, mean \pm SEM, * P < 0.01). (C) DKO mice received 20 IP injection of Stattic at a concentration of 20mg/kg every other day or the vehicle DMSO. qPCR-RT analysis showed significant reduced expression Stat3 target genes, but not Yap/Taz target genes (n=3, mean \pm SEM, * P < 0.05). (D) Representative macroscopic appearance of livers treated with DMSO or Stattic. (E) Quantitative analysis of liver-to-body weight ratio (n=5 for DMSO and n=3 for Stattic). Data are expressed as the mean \pm SEM. * P < 0.05, ** P < 0.01, by 2-tailed Student t test (C and E) and 1-way ANOVA with Tukey's post-hoc test (A and B).



Supplementary Figure 12. Specific loss of Mst1 and Mst2 in Sox9⁺ cells results in bile duct hyperplasia but not tumor formation. (A) 4 weeks old *Sox9-CreERT2;Mst1⁻¹;Mst2^{fl/fl}* were injected with 0.2mg/g tamoxifen in peritoneal cavity. 6-month post injection, the mice were euthanized and used for analysis. EpCAM staining was performed on liver sections of these mice. Scale bars, 50 μ m. (B) EpCAM staining was performed on the DKO livers of 2month old mice. Scale bars, 50 μ m. (C) Three mice per genotype were used for the quantitation. 10 fields of view (n=3). (D) Quantification for phosphor-Histone3⁺(pH3⁺) cells per EpCAM⁺ cells (n=3). IF staining as indicated. Scale bars, 50 μ m. Data are expressed as the mean \pm SEM. * $P < 0.05$, ** $P < 0.01$, by 2-tailed Student t test